◻   411

An Optimal HSI Image Compression using DWT and CP

D. Narmadha, K. Gayathri, K. Thilagavathi, N. Sardar Basha
Departement of Electronics and Communication Engineering, C. Abdul Hakeem College of Engineering and
Technology, Vellore, India

Article Info	ABSTRACT
	The compression of hyperspectral images (HSIs) has recently become a very attractive issue for remote sensing applications because of their volumetric data. An efficient method for hyperspectral image compression is presented. The proposed algorithm, based on Discrete Wavelet Transform and CANDECOM/PARAFAC (DWT-CP), exploits both the spectral and the spatial information in the images. The core idea behind our proposed technique is to apply CP on the DWT coefficients of spectral bands of HSIs. We use DWT to effectively separate HSIs into different sub-images and CP to efficiently compact the energy of sub-images. We evaluate the effect of the proposed method on real HSIs and also compare the results with the well-known compression methods. The obtained results show a better performance when comparing with the existing method PCA with JPEG 2000 and 3D SPECK.

Corresponding Author:

D. Narmadha,
Departement of Electronics and Communication Engineering,
C.Abdul Hakeem College of Engineering, Vellore, India.
Email: srinana1822@gmail.com

1.   INTRODUCTION

Hyperspectral images are used in different practical applications such as the detection of the earth's surface, soil type analysis, agriculture and forest monitoring, environmental studies and so on [1].

There are two types of redundancy in the HSIs i.e. spatial and spectral redundancies. However, the spectral correlation (band redundancy) is generally but not always stronger than spatial correlation [2]. Several compression methods have recently been proposed which can be classified into two main types as lossless and lossy compression methods. Lossless compression can only provide limited compression ratios, and the maximum achievable order is around three times (3:1) [3]. This ratio is not a reasonable value in many practical applications, especially in remote sensing.

Traditional compression algorithms for HSIs have only considered the spectral value in a feature space whose dimensions were spectral bands. Then, dimension reduction was often applied (by means of Principal Component Analysis (PCA) or Independent Component Analysis (ICA) [4]. However, they did not consider the spatial correlation when focusing on the spectral decorelation.

Therefore, 3D wavelet-based techniques such as Set Partitioning in Hierarchical Tress (SPHIT) algorithm and and Set Partitioned Embedded block (SPECK) for hyperspectral image compression have been proposed to exploit a joint consideration of the spatial and spectral correlations [5]. It has been shown in [5] that 3D-SPECK is better than 3D-SPIHT to achieve an efficient compression. In [6], a PCA-based method in conjunction with JPEG2000 for compressing HSIs was introduced. The results reveal that the performance of the method is superior to that of the spectral DWT, and the best PCA performance occurs when a reduced number of PCs are retained and encoded. Another compression algorithm based on JPEG2000 for HSIs was proposed in [7]. The algorithm can be applied for lossy and near-lossless compression applications in one single tool. It was also shown that the proposed scheme has a negligible effect on the results of selected applications (e.g., hard classification, spectral unmixing, and anomaly detection). In [8] a new lossy-to-

lossless coder based on 3D Tarp-based Coding with classification for Embedding (TCE) coupled with the reversible integer-valued Karhunen-Loève Transform (KLT) was introduced. The proposed method closely matches the lossy performance of JPEG2000 and outperformed JPEG2000 at lossless compression. An HSIs compression method based on band-of interest BOI-preserving- based was proposed in [9]. Some bands of HSIs are more important in the specific applications, and BOI selection methods can be chosen according to application requirements. BOI and non-BOI bands are respectively compressed with low distortion and high distortion. In [10] the impact of lossy compression on spectral unmixing and supervised classification using Support Vector Machine (SVM) was investigated. It was shown that for certain compression techniques, a higher compression ratio (CR) may lead to more accurate classification results. A new group and region based parallel compression method for hyperspectral imagery was proposed in [11].

Some compression methods currently consider HSIs as 3D data. Those compression methods are called a third-order tensor: two spatial dimensions and one spectral dimension. They try to take into account the spatial and spectral correlation of HSIs simultaneously and not alternatively as is the case for the above techniques [13]. Several tensor decompositions have been introduced in [14]. One of the most popular tensor decompositions is the Canonical decomposition (CP), which has been used for the compression of HSIs. CP allows the selection of any values for each dimension of the core tensor, which will be defined as $J_1 X J_2 X J_3$ in the next section and helps to obtain a higher compression ratio.
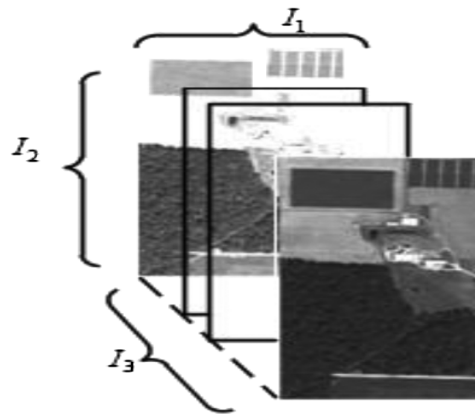

Figure 1. Third-dimension modeling of HSIs.

We propose a new HSIs compression algorithm based on discrete wavelet transform (DWT) and CP. Applying 2DWT to each spectral band will take care of first stage compression by using the (9/7) biorthogonal wavelet. Next, CP is applied to the four wavelet sub-images of the HSIs in order to achieve more CR. Finally, adaptive arithmetic coding (AAC) is used for coding the elements of the core tensors.

We compare the proposed method with the best known techniques, such as the 3D-SPECK algorithm [5], and both PCA and JPEG2000 [6]. Our experimental results over the two most used HSIs (AVIRIS datasets: Cuprite and Moffett Field) demonstrate and confirm the effectiveness of our algorithm in providing a much smaller MSE for the desired set of CRs, especially when the CR is selected higher than 160, in this case the performance of the proposed algorithm is significantly better than the other techniques. The proposed method also increases the pixel-based supervised classification accuracy.

2. 3D REPRESENTATION OF HYPERSPECTRAL IMAGES

HSIs are the images generated by the imaging spectrometer by collecting image data simultaneously in hundreds of spectral bands or frequencies (e.g. 5–10 nm spectral width) that reach a nearly contiguous spectral record. The large amount of bands increases the complexity and time of processing. HSIs can be represented as a third dimensional data $\underline{X} \in R^{I_1 X I_2 X I_3}$ as shown in Figure 1.

Unlike natural images, HSIs have two types of correlation simultaneously, which are the spatial correlation within images and the spectral correlation between spectral bands. The spectral correlation is generally stronger than spatial correlation. The average correlation coefficient between two spectral bands of 3D-data cube can be measured as follows:

For $i_3 = 1$ to $I_3 = 1$

$$\rho(i_3) = \frac{cov\ (\underline{X}\ (:,:,i_3),\ \underline{X}(:,:,i_3 + 1))}{\sqrt{var(\underline{X}\ (:,:,i_3)),}\ \ \sqrt{var\underline{X}(:,:,i_3 + 1))}}$$

End $\overline{p} = \frac{1}{I_3 - 1}\sum_{i_3=1}^{I_3 - 1}\rho(i_3)$ (1)

In most HSIs datasets, such as AVIRIS data cube, the value of is higher than 0.90 which means that the spectral correlation among bands is very high.

Exploiting both of spectral and spatial correlations is the key for the success of a compression algorithm. In this paper, a hybrid scheme based on DWT and CP for compression of HSIs is introduced. DWT and CP are briefly introduced in the next sections.

2.2. Discrete Wavelet Transform (DWT)

The DWT has successfully been used in many image processing applications including noise reduction, edge detection, and compression [15]. Indeed, the DWT is an efficient decomposition of signals into lower resolution and details. From the the deterministic image processing point of view, DWT may be viewed as successive low-pass and high-pass filtering of the discrete time-domain signal. At each level, the high pass filter produces detailed information (horizontal (H), vertical (V) and diagonal (D) information), while the low pass filter associated with scaling function produces the approximate (A) information. We apply a two dimensional DWT to each band of HSIs. If each image band has rows and columns, then after applying the 2DWT, we obtain four sub-band images (A, H, V, D), each having $I_1/2$ rows and $I_2/2$ columns. The A sub-band images have the highest energy among all the coefficients of the other sub-band images.

The 2DWT of function $f(x, y)$ with of size I_1 and I_2 can be shown as

$$W\varphi(i_1, i_2) = \frac{1}{\sqrt{I_1 I_2}}\sum_{y=0}^{I_2-1}\sum_{x=0}^{I_l-1} f(x, y)\varphi_{i_1,i_2}(x, y) \qquad\qquad (2)$$

$$W_{\psi}^{k}(j, i_1, i_2) = \frac{1}{\sqrt{I_1 I_2}}\sum_{y=0}^{I_2-1}\sum_{x=0}^{I_l-1} f(x, y)\varphi_{j,\ i_1,i_2}^{k}(x, y) \qquad\qquad (3)$$

$$k = \{H, D, V\} \qquad\qquad (4)$$

$$\begin{aligned}\varphi_{i_1,i_2}(x, y) &= \varphi(x - i_1, y - i_2) \\ &= \sum_m h_{\varphi}(m - 2i_1)\sqrt{2}\,\varphi(2x - m) \\ X\ \sum_n h_{\varphi}\,(n - 2i_2)\,\sqrt{2}\,\varphi(2x - n)\end{aligned} \qquad\qquad (5)$$

$$\begin{aligned}\psi_{j,i_1 i_2}^{H}(x, y) &= 2^{\frac{i}{2}}\psi^{H}(2^j x - i_1, 2^j y - i_2) \\ &= 2^{\frac{i}{2}}\sum_m h_{\psi}(m - 2i_1)\sqrt{2}\,\psi(2^{j+1}x - m) \\ &\quad X\ \sum_n h_{\psi}\,(n - 2i_2)\,\sqrt{2}\,\psi(2^{j+1}x - n)\end{aligned} \qquad\qquad (6)$$
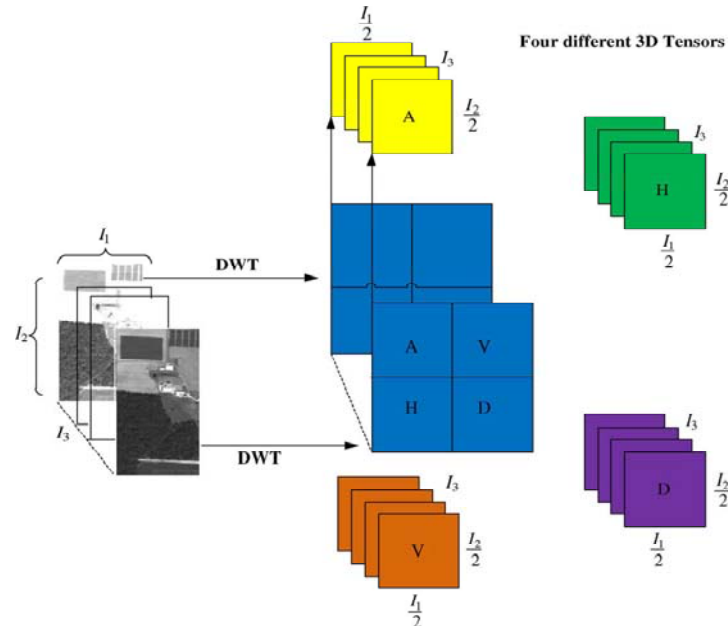
Figure 2. New decomposition scheme for HSIs.

Table 1. 9/7 Biorthogonal Wavelet Filter

N	$h_\varphi[n]$	$h_\psi[n]$
0	0.7885	0.8527
±1	0.4181	0.3774
±2	-0.04069	-0.111
±3	-0.06454	-0.02385
±4		0.03783

φ is called scaling function. The $W_\varphi(i_1, i_2)$ coefficients define an approximation of (x, y). The $W_\psi(j, i_1, i_2)$ coefficients add horizontal, vertical and diagonal details. Normally $i_1 = i_2 = 2^j$ is selected and so that $j = 0,1,2, \dots, J-1$ [16]. The h_φ and h_ψ are called wavelet filters. For the choice of wavelet filtering, the (9/7) biorthogonal wavelet which is used in JPEG2000, is selected in order to improve the compression ratio [17]. Filter coefficients of (9/7) biorthogonal wavelet are shown in Table 1 [18], [19].

The inverse 2D-DWT is given by,

$$f(x,y) = \frac{1}{\sqrt{I_1 I_2}} \sum_{i_2} \sum_{i_1} w_\varphi(i_1, i_2) \varphi_{i_1, i_2}(x, y)$$
$$+ \frac{1}{\sqrt{I_1 I_2}} \sum_{k=\{H,D,V\}} \sum_{j=0}^{J-1} \frac{1}{\sqrt{I_1 I_2}} \sum_{i_2} \sum_{i_1} w_\psi^k(i_1, i_2) \psi_{j, i_1, i_2}^k(x, y) \tag{7}$$

In lossy compression, we can ignore the detailed sub-bands (for example H, V and D) or preserve only important detailed information. In order to achieve a higher compression ratio, we can still decompose the images in more than one level.

B. Nonnegative Tensor Decomposition
    In this section a brief review of the tensor model is presented. Important notations are shown in Table 2.
    The third-order TD tensor is described as a decomposition of a given third order tensor $\underline{Y} \in R^{I_1 \times I_2 \times I_3}$ into an unknown core tensor $\underline{G} \in R^{I_1 \times I_2 \times I_3}$ multiplied by a set of three unknown component matrices where $A^{(n)} = a_1^{(n)}, a_2^{(n)}, \dots \dots a_{J_n}^{(n)} \in R^{I_n \times J_n}$ (n = 1, 2, 3), represent common factors [20].

Table 2. Notations of Tensor Decomposition

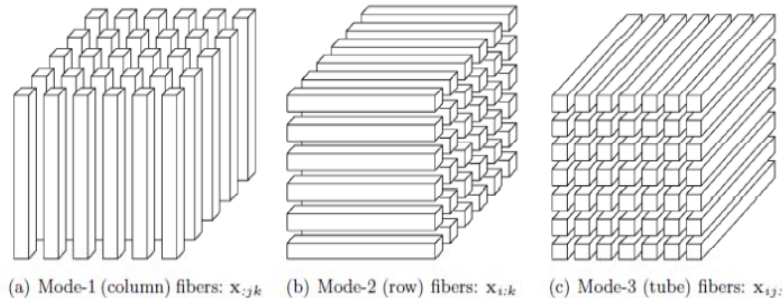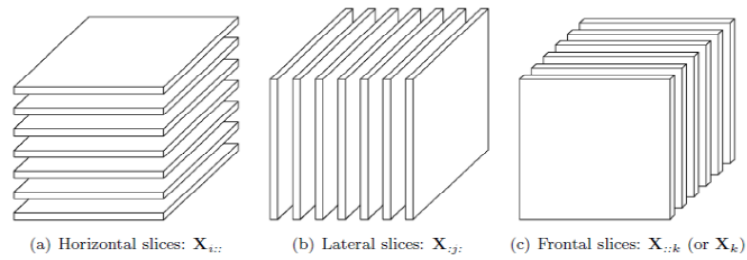| Notation	Description
R^n	n-dimensional real vector space
Y	Third order Tensor
$Y^{(n)}$	n-mode matricization of tensor Y
$A^{(n)}$	n-mode matrix in tucker model
∘	Outer product
X_n	n-mode product of a tensor by matrix

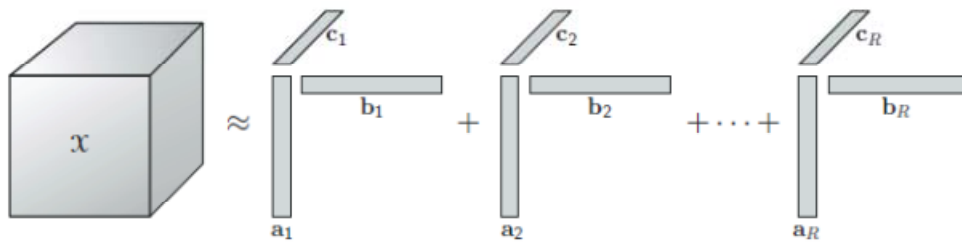Figure 3. Fibers of the 3-order tensor

Figure 4. Slices of a 3-order tensor

Figure 5. CP decompositionof a 3 way array

The CP decomposition factorizes a tensor into a sum of component rank-one tensors. For example, given a third-order tensor $\mathbf{X} \approx R^{I \times J \times K}$, we wish to write it as
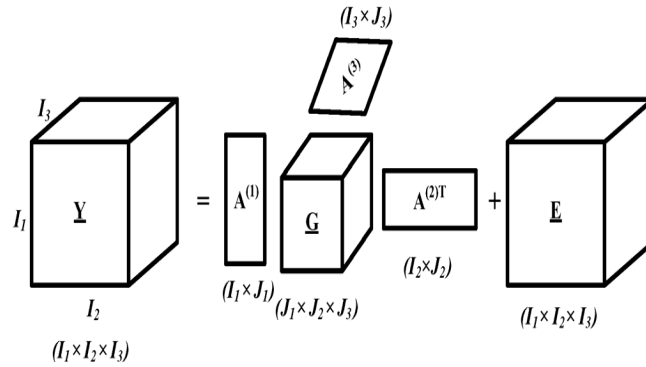
$$\mathbf{X} \approx \sum_{r=1}^{R} a_r \circ b_r \circ c_r$$

Figure 6. Third order Tensor Decomposition

$$\underline{Y} = \sum_{j_1-1}^{J_1} \sum_{j_2-1}^{J_2} \sum_{j_3-1}^{J_3} g_{j_1 j_2 j_3} \; a_{j_1}^{(1)} \, o \; a_{j_2}^{(2)} \, o \; a_{j_3}^{(3)} + \underline{E}$$
$$= \underline{G} \; x_1 \, A^{(1)} \, x_2 \, A^{(2)} \; x_3 \, A^{(3)} + \underline{E}$$
$$= \underline{G} \; x \{A\} + \underline{E} = \hat{\underline{Y}} + \underline{E} \tag{8}$$

Here tensor is an estimation of tensor, and it depends on the values, which are the dimensions of the core tensor, and tensor denotes the estimation error. Most algorithms for the Nonnegative Tensor Decomposition (NTD) model are based on Alternative Least Square (ALS) minimization of the squared Euclidean distance used as a global cost function subject to nonnegative constraints, that is:

$$D_F \big(\underline{Y} \; \| \; \underline{G} \, \{A\} \big) = \frac{1}{2} \, \| \underline{Y} - \hat{\underline{Y}} \|^2 \tag{9}$$

Here the objective is to find the optimal component matrices $A^{(n)} \in R^{I_n \times J_n}$ and the core tensor $\underline{G} \in R^{I_1 \, X \, I_2 \, X \, I_3}$.

Almost all the existing algorithms for Tensor decompositions [12] require certain processing based on the full tensor during the estimation. The real-world data often contain millions of elements. Full data processing (such as the inverse computation) is therefore impractical. We use the Hierarchical Nonnegative Tensor Decomposition algorithm in proposed method.

3. PROPOSED COMPRESSION ALGORITHM

The compression is performed using four steps. In the first step, 2DWT is applied to each spectral band of the HSIs in order to obtain 4 sub-images (approximate, diagonal, vertical and horizontal) for each spectral band (see Figure 2). In the second step, the CP algorithm is applied to the four tensors. For each tensor, the size of the core tensor $\underline{G}$, i.e. (J_1, J_2, J_3), was selected manually. The approximate tensor has the lowest frequency components containing most of the wavelet coefficient energy, so the values of (J_{1A}, J_{2A}, J_{3A}) were set higher than those of other tensors. The values of (J_{1D}, J_{2D}, J_{3D}) for the diagonal tensor, which contains the diagonal information, were also set higher than the (J_{1H}, J_{2H}, J_{3H}) and (J_{1V}, J_{2V}, J_{3V}) values of horizontal and vertical tensors.

3.1. Computing CP Decomposition.

As mentioned previously, there is no finite algorithm for determining the rank of a tensor [143, 101]; consequently, the first issue that arises in computing a CP decomposition is how to choose the number of rank-one components. Most procedures fit multiple CP decompositions with different numbers of components until one is "good." Ideally, if the data are noise-free and we have a procedure for calculating CP with a given number of components, then we can do that computation for $R = 1, 2, 3, \ldots$ components and stop at the first value of R that gives a fit of 100%.

Assuming the number of components is fixed, there are many algorithms to compute a CP decomposition. Here we focus on what is today the "workhorse" algorithm for CP: the alternating least squares (ALS) method proposed in the original papers by Carroll and Chang [38] and Harshman. For ease of

presentation, we only derive the method in the third-order case, but the full algorithm is presented for an N-way tensor in Figure 3

CR in this step can be considered as the ratio between the total number of bits in the original input data, and the number of bits must be transmitted and is shown as

$$CR = \frac{(I_1 \, x I_2 \, x I_3 \,)}{B}$$

$$B = \frac{I_1}{2} \, x \, J_{1A} + \frac{I_2}{2} \, x \, J_{2A} + I_3 \, x \, J_{3A} + J_{1A} x \, J_{2A} \, x \, J_{3A}$$

$$+ \frac{I_1}{2} \, x \, J_{1D} + \frac{I_2}{2} \, x \, J_{2D} + I_3 \, x \, J_{3D} + J_{1D} x \, J_{2D} \, x \, J_{3D}$$

$$+ \frac{I_1}{2} \, x \, J_{1V} + \frac{I_2}{2} \, x \, J_{2V} + I_3 \, x \, J_{3V} + J_{1V} x \, J_{2A} \, x \, J_{3V}$$

$$+ \frac{I_1}{2} \, x \, J_{1H} + \frac{I_2}{2} \, x \, J_{2H} + I_3 \, x \, J_{3H} + J_{1H} x \, J_{2H} \, x \, J_{3H} \qquad (10)$$

In the third step, the 4 core tensors $\underline{G}$ and 12 matrices should be transmitted.

Most elements of the core tensors $\underline{G}$ (especially diagonal, vertical and horizontal core tensors) are nearly zero. The bitplane coding procedure is used to transmit the elements of these core tensors $\underline{G}$. The bitplane coding includes two passes: the significant pass and the refinement. First, we define a significant map of a given threshold T and the element $g_{j_1 j_2 j_3}$. Suppose $|g_{j_1 j_2 j_3}$ represents the absolute value of the core tensor element at the location (j_1, j_2, j_3) and $s_{j_1 j_2 j_3}$ represents the significant state for the threshold T (where T is an integer power of 2).

$$s_{j_1 j_2 j_2} = \begin{cases} 1 & T \leq |g_{j_1 j_2 j_2}| \leq 2T \\ 0 & O.W \end{cases} \qquad (11)$$

For $s_{j_1 j_2 j_3} = 1$, the $g_{j_1 j_2 j_3}$ is considered as the significant element. The significant element must be encoded and removed from the core tensor, and the insignificant elements are preserved for the next bitplane. After that, the significant threshold is divided in half, and the process is repeated for the next pass. This process is repeated until the energy of the encoded elements equal to or higher than 99.5% of that of the original core tensor. The selected elements and their positions must be transferred. There are many possible approaches for coding a significant map. Most wavelet-based coders use adaptive arithmetic coding (AAC) for lossless entropy coding. We also use AAC for coding the significant element. Arithmetic coding is a variable-length lossless coding. Arithmetic coding does not require the transmission of codebook and so achieves a higher compression than Huffman coding. Arithmetic coding essentially amounts to computing the cumulative distribution function (CDF) of the probability of a sequence of symbols and then representing the resulting numerical value in a binary code.

The columns of matrices $A^{(n)}$ are called $a_{j_n}^{(n)}$ in the proposed algorithm, which are normalized vectors. The absolute value of $a_{j_n}^{(n)}$ elements are in the range [0, 1], and they are very close to each other. Therefore, in order to transfer the 12 matrices $A^{(n)}$, a uniform quantization is used. In the fifth step, the transmitted data are decoded. Finally in the sixth step, the inverse of 2DWT is applied to reconstruct the images.

3.2. Proposed Algorithm (DWT-CP)
3.2.1. Proposed Algorithm for Coder
Input: Original HSIs $\underline{X}$ (the size $I_1 x \, I_2 x \, I_3$)
1-Apply DWT to each spectral band to obtain 4 sub-images (approximate, diagonal, vertical and horizontal tensors).
2-Apply CP algorithm to the four tensors individually. Each tensor has the size of ($I_1/2 \, x \, I_2/2 \, x \, I_3$)

Input: Data tensor Y: ($I_1 \times I_2 \times \cdots \times I_N$), rank R,
Unfolding rule $\mathbf{l} = [\mathbf{l}_1, \mathbf{l}_2, \ldots, \mathbf{l}_M]$ where $\mathbf{l}m = [lm(1), \ldots, lm(Km)]$

Output: $\lambda \in \mathrm{R}^N$, N matrices $\mathbf{A}^{(n)} \in \mathrm{R}^{In \times R}$
Begin

Stage 1:
$$\|g, U^{(1)}, \ldots, U^{(M)}\| = TD(y_{[l],} \min(I, R))$$

Stage 2:
$$\|\lambda; B^{(1)}, ..., B^{(M)}\| = CPD(g, R)$$

$$for\ m = 1,2, ... M\ do\ B^{(m)} \leftarrow U^{(m)} B^{(m)}$$
$$for\ m = 1,2, ... M\ do$$
$$for\ r = 1,2, ..., R\ do$$
$$\|g, a_r^{(l_{m1})}, ..., a_r^{(l_{mk})}\| = TD(reshape(b_r^{(m)}, [I_{l_{m(1)}}, ..., I_{l_{m(K_m)}}]), 1)$$
$$\lambda_r \leftarrow \lambda_r g$$

End CP

4-Quantize $A^{(n)} \in R^{I_n \times J_n}$ and encode core tensor $\underline{G} \in R^{I_1 \times I_2 \times I_3}$ Using AAC

3.2.2. Proposed Algorithm for Decoder
5-Decode the elements $\underline{\bar{Y}} = \underline{\bar{G}} \times \{\hat{A}\}$
6-Calculate the inverse 2DWT to reconstruct images.
Output: Reconstructed images $\underline{\hat{X}}$.

4.   COMPUTATIONAL COMPLEXITY

In the following, we analyze the complexity of the algorithm. We considered an -tap filter bank and denoted L_b as the number of wavelet decomposition levels in the spatial band. The complexity of applying 2DWT to the tensor $\underline{X}$ with the size of $I_1 x\ I_2 x\ I_3$ is O($8NI_1I_2\ I_3$ $(1-2^{-2\ L_b})$ / 6). In the proposed algorithm we are using the (9/7) wavelet and also one level of decomposition, so the complexity of our algorithm is O($9I_1I_2\ I_3/7$).

After applying 2DWT, each tensor (approximate, diagonal, vertical and horizontal tensors) has the size of $(I_1/2)\ X\ (I_2/2)\ X\ I_3$. The max complexity of the TD is of order O($J_A I_A^3$), where I_A is the average number of pixels of the approximate tensor, and J_A is the average of the dimensions of the approximate core tensor $\underline{G}$.

Table III. SNR(dB) VALUES FOR, DWT-CP, PCA+JPEG2000, 3D- SPECK

Method	Bpppb				
	0.05	0.1	0.2	0.5	1.0
Cuprite					
DWT-CP	49.9	52.9	53	54.9	58.8
DWT-TD	49.5	52.1	52.6	54.2	58.1
PCA+JPEG 2000	43.1	45.3	48.2	50.5	54.2
3D SPECK	34.7	37.1	40.8	46.6	50.1
Moffett Field					
DWT-CP	42.6	43.9	48.1	52.5	55.9
DWT-TD	40.1	43.7	47.8	51.3	55.3
PCA+JPEG 2000	34.7	39.3	43.6	47.2	51
3D SPECK	24.3	28.2	32.3	39.6	45.1

$$I_A = \frac{1}{3}\left(\frac{I_1}{2} + \frac{I_2}{2} + I_3\right) \tag{12}$$

$$J_A = \frac{1}{3}(J_{1A} + J_{2A} + J_{3A}) \tag{13}$$

Therefore, the total complexity of the proposed algorithm (DWT-CP) is of order 4 x O($J_A I_A^3$)+O($9I_1I_2\ I_3/7$).

5. EXPERIMENTAL RESULTS

5.1. Compression Results

To measure the perceptual quality of images, the signal-to-noise ratio (SNR) can be well used. It actually estimates the quality of the reconstructed images $\hat{\underline{X}}$ in comparison with the original ones $\underline{X}$. The SNR in dB is defined as

$$SNR_{dB} = 10 \ log_{10} \left(\frac{\|\underline{X}\|^2}{\|\underline{X} - \hat{\underline{X}}\|^2} \right) \tag{14}$$
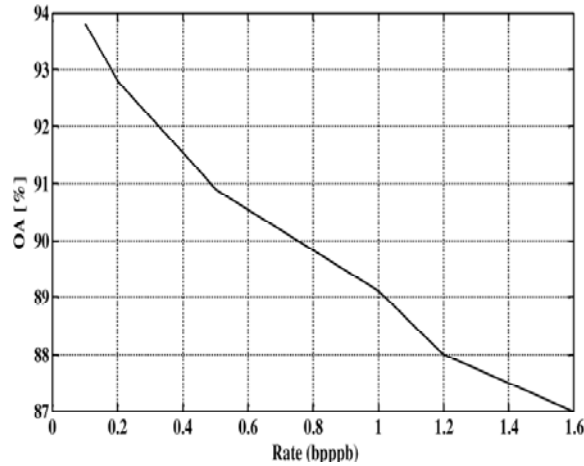
Figure 7. Classification accuracy of DWT-CP using SVM (RBF Kernel).

Where $\|\underline{X} - \hat{\underline{X}}\|^2 = \sum_{k=1}^{I_3} \sum_{j=1}^{I_2} \sum_{i=1}^{I_1} \left(x_{ijk} - \hat{x}_{ijk} \right)^2$.

Two popular AVIRIS datasets (Cuprite and Moffett) are used in our experiments. 2 These 16-bit radiance datasets have been cropped spatially to a size of 512 x 512 and composed of 224 spectral bands.

First, we apply the proposed algorithm (DWT-CP) to these images. Next, we compare the SNRs achieved by the proposed algorithm with those obtained from the well-known techniques, i.e. 3D-SPECK algorithm [5], combined PCA+JPEG2000 [6] on a set of HSIs. Table III shows the SNR versus different bpppb for the Cuprite and Moffett HSIs. In our experiments, DWT-CP has significantly improved SNR at high CRs (small bpppbs) especially when the CR is higher than 160 or bpppb is lower than 0.1.
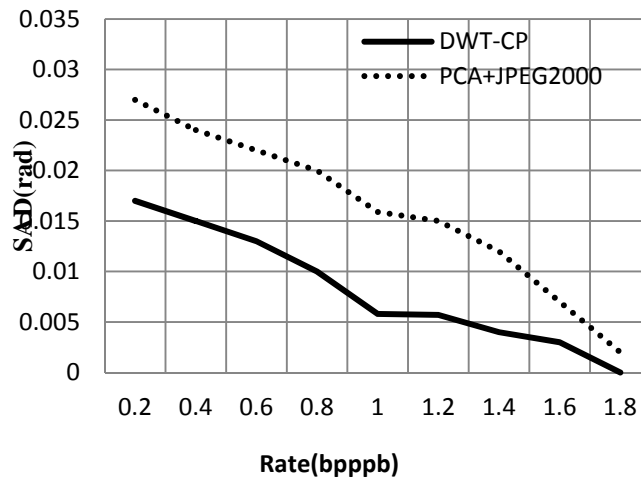

Figure 8. SAD (Rad) versus bpppb for, DWT-CP and JPEG2000.

6.   CONCLUSION

In this paper, we introduced a new method for HSIs compression using DWT and CP. This is carried out by reducing the size of 3D tensors computed from four wavelet sub-images of the spectral bands of HSIs. The performance of the proposed algorithm on AVIRIS datasets yields the following results:

1) DWT-CP achieves higher SNR in comparison with two state-of-art algorithms (3D-SPECK algorithm and combined PCA+JPEG2000) especially at bpppb lower than 0.1.
2) The proposed algorithm achieves a better pixel-based SVM classification accuracy.

REFERENCES

[1] H.F. Grahn and P. Geladi, Techniques and Applications of Hyperspectral Image Analysis. Chichester, U.K.: Wiley, 2007.
[2] C.Huo, R. Zhang, and T. Peng, "Lossless compression of hyperspectral images based on searching optimal multibands for prediction", *IEEE Geosci. Remote Sens. Lett*. vol. 6, no. 2, pp. 339–343, Apr. 2009.
[3] J. Serra-Sagristà and F. Aulí-Llinàs, "*Remote sensing data compression*", in Computational Intelligence for Remote Sensing. Berlin, Germany: Springer-Verlag, Jun. 2008, pp. 27–61.
[4] J.Wang and C. Chang, "Independent component analysis-based dimensionality reduction with applications in hyperspectral image analysis", *IEEE Trans. Geosci. Remote Sens*., vol. 44, no. 6, pp. 1586–1600, Jun.2006.
[5] X. Tang andW. A. Pearlman, "*Three-dimensional wavelet-based compression of hyperspectral images*", in Hyperspectral Data Compression, G. Motta, F. Rizzo, and A. Storer, Eds. : Springer, 2006, ch. 10,pp. 273–278.
[6] Q. Du and J. E. Fowler, "Hyperspectral image compression using JPEG2000 and principal component analysis", *IEEE Geosci. Remote Sens. Lett*., vol. 4, no. 2, pp. 201–205, Apr. 2007.
[7] G. P. Abousleman, M. W. Marcellin, and B. R. Hunt, "Compression of hyperspectral imagery using the 3-D DCT and hybrid DPCMDCT", *IEEE Trans. Geosci. Remote Sens*., vol. 33, no. 1, pp. 26–34, Jan. 1995.
[8] J. Robinson and V. Kecman, "Combining support vector machine learning with the discrete cosine transform in image compression", *IEEE Trans. Neural Networks*, vol. 14, no. 4, pp. 950–958, Jul. 2003.
[9] F. Garcia-Vilchez, J. Munoz-Mari, and I. B. M. Zortea et al., "On the impact of lossy compression on hyperspectral image classification and unmixing", *IEEE Geosci. Remote Sens. Lett*., vol. 8, pp. 253–257,Mar.2011.
[10] L. Chang, C.Yang-Lang, and Z. S. Tang et al., "Group and region based parallel compression method using signal subspace projection and band clustering for hyperspectral imagery", *IEEE J. Sel. Topics Appl. Earth Observ. Remote Sens*., vol. 4, no. 3, pp. 565–578, Sep. 2011.
[11] L. Santos, S. Lopez, and G. M. Callico et al., "Performance evaluation of the H.264/AVC video coding standard for lossy hyperspectral image compression," IEEE J. Sel. Topics Appl. Earth Observ. Remote Sens., 2012.
[12] W. Kim and C.-C. Li, "*A study on oreconditioning multiwavelet systems for image compression*", inWavelet Analysis and Its Applications, Y. Y. Tang, P. C. Yuen, and C.-H. Li, Eds. New York: Springer, 2001,pp. 22–36.
[13] A. Cohen, I. Daubechies, and J.-C. Feauveau, "Biorthogonal bases of compactly supported wavelets", *Commun. Pure and Appl. Math*., vol. 45, no. 5, pp. 485–560, May 1992.
[14] M. Antonini, M. Barlaud, and P. Mathieu et al., "Image coding using wavelet transform", *IEEE Trans. Image Process*., vol. 1, no. 2, pp. 205–220, Apr. 1992.
[15] A. Cichocki, R. Zdunek, and A. H. Phan et al., *Nonnegative Matrix and Tensor Factorizations*. Chichester, U.K.:

BIOGRAPHIES OF AUTHORS

D. Narmadha received B.E (ECE) in Ranganathan Engineering College, Coimbatore. She is currently pursuing Master of Engineering in Applied Electronics, C.Abdul Hakeem College of Engineering and Technology Melvisharam.
She has presented many papers in National and International Conferences. She attended workshop in Implementational Aspects of Microcontrollers. Her Area of research includes Image Processing, Networking, Embedded System. She ia an active member of IETE.

K. Gayathri graduated her B.E. in Electronics and communication engineering from C.Abdul Hakeem College of Engineering and Technology, Melvisharam. She is currently pursuing the M.E. (Applied Electronics) from C.Abdul Hakeem College of Engineering and Technology, Melvisharam.
She has published many papers in National and International conference proceedings. She attended many workshops in SCARA Robots, Robotics and embedded system design. Her research interests include Image Processing, Embedded system Design, Pattern Recognition and Multiscale methods in image processing. She is an active member of IETE.

K. Thilagavathi Started Career towards Engineering in 2011 as B.E (ECE) student. She is curretly doing Master of Engineering in Applied Electronics at C.Abdul Hakeem College of Engineering and Technology, Melvisharam.
She attended many workshop in Embedded System and VLSI domains. She has presented in many national and International conferences. Her Area of interest includes Image Processing, VLSI, Embedded System Design, Verilog, Networking. She ia an active member of IETE.